

# Mechanism of the screw-sense reversal of tightly hydrogen-bonded $\alpha$ -helical network triggered by the side-chain conformation

Akihiro Abe<sup>a,\*</sup>, Yosuke Imada<sup>a</sup>, Hidemine Furuya<sup>b</sup>

<sup>a</sup>Nano-Science Research Center, Tokyo Polytechnic University, Iiyama, Atsugi 243-0297, Japan

<sup>b</sup>Department of Organic and Polymeric Materials, Tokyo Institute of Technology, Ookayama, Meguro-ku, Tokyo 152-8552, Japan

## ARTICLE INFO

### Article history:

Received 18 July 2010

Received in revised form

13 October 2010

Accepted 23 October 2010

Available online 3 November 2010

### Keywords:

Reversal of  $\alpha$ -helix sense

Conformational energy difference of side chains

Two-parameter zipper theory

## ABSTRACT

The paper presents theoretical treatment of a screw-sense reversal of tightly hydrogen-bonded  $\alpha$ -helical polypeptide chains. The transition is triggered by the conformational free-energy difference ( $s$ ) of the side chain flanking the chiral (right( $r$ )- or left( $\ell$ )-handed) backbone. The two-parameter scheme ( $s$ ,  $\sigma$ ) corresponding to a zipper-type transition model starting from one terminal has been constructed and applied to the thermally-induced helix–helix transition characteristic of polyaspartic acid esters observed in the helicoidal solution. The weighting parameter  $\sigma$  takes care of the instability associated with the  $\ell/r$  junction, i.e., the unfolded site where at least three successive hydrogen-bonds should become free to change their partner. The enthalpy of transition (ca. 2 kJ/mol) of poly( $\beta$ -phenethyl  $L$ -aspartate) (PPLA) ( $M_v = 6 \times 10^4$ ) observed in the lyotropic liquid crystalline state in 1,1,2,2-tetrachloroethane has been reproduced with the instability parameter  $\sigma = 0.001$ – $0.0001$ . Attempts were further extended to interpret the thermally-induced helix–helix transition behaviors of the PPLA homopolymers and random copolymers involving benzyl  $L$ -aspartate residues observed under various conditions.

© 2010 Elsevier Ltd. All rights reserved.

## 1. Introduction – a short description of the background

Under certain conditions, polypeptides that are capable of adopting two  $\alpha$ -helical forms, i.e., right( $r$ )- and left( $\ell$ )-handed screw, may undergo a sharp conformational transition. (In the following, symbols  $r$  and  $\ell$  will serve in two capacities: i.e., representing either the screw-sense of an  $\alpha$ -helix or the handedness of a given unit constituting the  $\alpha$ -helical array.) Blout et al. [1,2] have first found that poly( $\beta$ -benzyl  $L$ -aspartate) (PBLA) has a helical sense opposite to that of more popular poly( $\gamma$ -benzyl  $L$ -glutamate) (PBLG) in chloroform solution. PBLA  $\alpha$ -helix normally takes the  $\ell$ -form, the  $r$ -form being reported only under certain limited conditions [3–8]. Goodman et al. [9] have demonstrated that random copolymers of  $\beta$ -benzyl and  $\beta$ -nitrobenzyl  $L$ -aspartate exhibit a sharp transition of the Moffitt  $b_0$  value in chloroform solution from positive for PBLA to negative for poly( $\beta$ -nitrobenzyl  $L$ -aspartate) (PNBLA) when plotted against the  $\beta$ -nitrobenzyl content. While PBLA prefers the  $\ell$ -helix, the most stable form of PNBLA is  $r$  at room temperature. Since then, the so-called helix–helix transition

has been widely recognized as a characteristic of polyaspartic acid esters [10–15].

These polymers are known to exhibit solvent-induced as well as thermally-induced helix–helix transitions depending on the polarity of the media and the chemical structure of the pendant side groups [9–18]. Scheme 1 is constructed to demonstrate briefly the phase transition behaviors of poly( $\beta$ -phenethyl  $L$ -aspartate) (PPLA). PPLA takes the  $\alpha$ -helical  $r$ -form in 1,1,2,2-tetrachloroethane (TCE) at moderate temperatures. The transition to the  $\ell$ -helix occurs at 85–90 °C in the isotropic solution as well as in the lyotropic liquid crystalline (LC) state [19]. In the presence of a denaturant acid, PPLA also exhibits a transformation to the  $\ell$ -form by lowering temperature. In Scheme 1, the two coil states which appear in the higher- and lower-temperature regions are also included [16,20–23]. Accordingly, a ternary mixture such as PPLA/TCE/trifluoroacetic acid (TFA) could possibly exhibit as many as five phases under a proper condition at a polarizing microscopic examination (the outermost framework of the scheme) [18]. PPLA is also known to undergo an irreversible helix–helix transition around 135 °C in the solid state [24]. On the contrary, PBLG is known to exist only in the  $r$ - $\alpha$ -helix in conventional helix-forming solvents as well as in bulk. As shown above, PBLG and PPLA are mutually isomeric in their chemical structures: i.e., PBLG can be converted into PPLA by interchanging a  $\gamma$ -CH<sub>2</sub> with the ester group in the side chain. The major difference

\* Corresponding author. Tel./fax: +81 45 563 4473.

E-mail address: [aabe34@xc4.so-net.ne.jp](mailto:aabe34@xc4.so-net.ne.jp) (A. Abe).



Since the reversal of the screw-sense takes place only at the moving front, parameter  $\sigma$  takes care of the instability associated with the  $\ell/r$  junction, i.e., the transition state where at least three successive H-bonds should become free to change their partner. In Scheme 2,  $\sigma$  is symbolically included to represent such an irregular event. The configurational partition function  $Z$  for an  $\alpha$ -helical rod of  $n$  units may be expressed by the matrix-multiplication scheme:

$$Z = J_0 M^n J_n \quad (2)$$

where

$$M = \begin{matrix} R & L \\ R & \begin{bmatrix} 1 & \sigma s \\ 0 & s \end{bmatrix} \\ L & \end{matrix} \quad (3)$$

and  $J_0$  and  $J_n$  are respectively the row and column vectors to collect the desired elements. For simplicity,  $n$  may be taken to be the degree of polymerization (DP). In this particular example, however,  $Z$  can be alternatively replaced by a simple algebraic expression such as

$$\begin{aligned} Z &= s^n + \sigma(s^{n-1} + s^{n-2} + \dots + s^2 + s) + 1 \\ &= s^n + \sigma \sum_{k=1}^{n-1} s^k + 1 \\ &= 1 + s^n + \sigma s(s^n - 1)/(s - 1) \end{aligned} \quad (4)$$

The fraction of  $\ell$ -unit in a given  $\alpha$ -helical array can be calculated by

$$\begin{aligned} f_{\text{left}} &= (1/n) \partial \ln Z / \partial \ln s \\ &= A/nB \end{aligned} \quad (5)$$

where

$$A = ns^n + \sigma s \left[ (n-1)s^n - ns^{n-1} + 1 \right] / (s-1)^2 \quad (6)$$

and

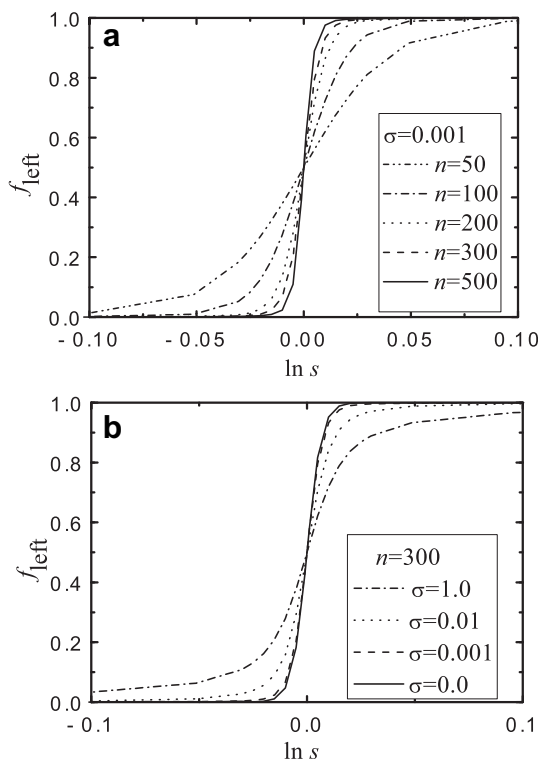


Fig. 2. (a)  $n$ -Dependence of transition curves calculated with  $\sigma = 0.001$ , and (b)  $\sigma$ -dependence of the transition curves for  $n = 300$ .

$$B = s^n + \sigma s(s^{n-1} - 1)/(s - 1) + 1 \quad (7)$$

In Fig. 2a, the effect of DP on the transition curves was examined at a fixed  $\sigma$  value (0.001) by plotting  $f_{\text{left}}$  against  $\ln s$  for various values of  $n$ . The slope becomes sharper as  $n$  increases. In the range  $n > 200$ , the variation of  $f_{\text{left}}$  becomes less sensitive with  $n$ . Alternatively, the  $f_{\text{left}}$  vs.  $\ln s$  plots calculated for various values of  $\sigma$  at  $n = 300$  are put together in Fig. 2b. The slope of the curve becomes sharper as  $\sigma$  decreases, approaching the limiting value in the range  $\sigma < 0.001$ . As manifestly shown by Eq. (4),  $\sigma$  is closely related to the fraction of the molecular species existing in the intermediate state. The average number of species containing the  $\ell/r$  junction is given by.

$$\begin{aligned} \nu &= \partial \ln Z / \partial \ln \sigma \\ &= \sigma \Sigma s^k / Z \\ &= 1 - (s^n + 1)/Z \end{aligned} \quad (8)$$

When  $\sigma = 0$ , the equilibrium should take place between the partitioned all  $r$ - and all  $\ell$ -form without any intermediate state. The value of  $\Delta H_c$  obtained under such an ultimate condition corresponds to the enthalpy change defined by the two-state equilibrium of the van't Hoff theory [39].

### 3. Analysis of the observed helix–helix transition data – elucidation of $\sigma$ and $\Delta H_c$

Shown in Fig. 3 is an example of the theoretical treatment of the experimental data of the screw-sense inversion of PPLA observed by  $^2\text{H}$  NMR in the LC state. The deuterium quadrupolar splittings due to the  $\beta_R$ -CD bond in the side chain varies sensitively with the helical sense of the backbone:  $\Delta\nu \approx 20$  kHz and 40 kHz, respectively, for the  $r$ - and  $\ell$ -regime. The relative intensity of these peaks can be used as a probe to follow the transition. The transition behaviors studied in this manner provides a basis to examine the validity of the theoretical framework (Eq. (1)–(7)). The computational procedure is as follows. (1) The values of  $s$  can be estimated by using Eq. (5)–(7) for given set of fraction-temperature data,  $\sigma$  being kept constant. In all calculations, the value of  $n$  may be set equal to 300 in consideration of the molecular weight ( $M_v = 6 \times 10^6$ ) of the sample. (2) The transition enthalpy,  $\Delta H_c$  is then obtained from the standard relation given in Eq. (1). (3) The process may be repeated for another possible choice of  $\sigma$ . In the example shown in Fig. 3, the experimental curve (filled circles) is well reproduced by the calculation (open circles) using a set of parameters such as  $\Delta H_c = 2.42$  kJ/mol and  $\sigma = 0.001$ .

The DSC measurements on PPLA solutions gave an estimate of the transition enthalpy in the range 1.5–1.8 kJ/mol for the LC state ( $\sim 25$  wt% in TCE). Although the DSC peaks are much broader, and thus less accurate for dilute isotropic solutions ( $\sim 5$  wt%), the

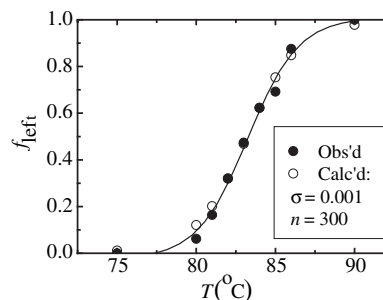


Fig. 3. Reproduction of experimental observations on PPLA (sample designated as E1) by theory. The transition enthalpy  $\Delta H_c$  thus estimated is 2.42 kJ/mol for the LC phase.

magnitude of the transition enthalpies estimated from the peak area was nearly identical with those for the more concentrated LC phase [40]. The conformational analysis of the  $^2\text{H}$  NMR data collected from PPLA carrying fully deuterated side chains gave an estimate of 1.1 kJ/mol for the energy difference between the two helical forms [32,35]. The side-chain conformation and the energy difference derived from  $^2\text{H}$  NMR measurements have been well reproduced by calculations such as MD simulation and rotational isomeric state (RIS) energy minimization [35].

Theoretical treatments were extended to include all other helix–helix transition data obtained by using the  $^2\text{H}$  NMR technique in the LC state. The results are accommodated in Table 1. In addition to the two independent measurements on the same PPLA homopolymer samples (E1, E2), copolymers comprising BLA and PLA [19] are also studied. In all cases, the deuterium atom introduced at the C- $\beta_{\text{R}}$  position of the side chain was used as a probe to detect the  $r \leftrightarrow \ell$  equilibration. The data adopted in the 4th row of the table were obtained from a 1:1 mixture of PPLA- $\beta_{\text{Rd}}$  and PBLG-Nd in a lyotropic LC state in TCE (25 wt%) [31]. Since the  $\alpha$ -helical PBLG remains in the rigid  $r$ -form over the entire temperature range, the  $r \leftrightarrow \ell$  helix-sense inversion of the guest (PPLA- $\beta_{\text{Rd}}$ ) should take place in a highly ordered LC environment of the host. The two experiments, with and without the host, yielded a comparable fraction vs. temperature plot characterized by the parameters such as (with)  $T_{\text{c}} = 86.6$  °C and the van't Hoff energy  $\Delta H_{\text{v}} = 503.0$  kJ/mol (the 4th row), and (without)  $T_{\text{c}} = 83.2$  °C and  $\Delta H_{\text{v}} = 656.2$  kJ/mol (the 2nd row) respectively. Essentially the same result was obtained from the experiment in which the host PBLG was replaced by poly( $\gamma$ -benzyl  $\text{D}$ -glutamate) (PBDG-Nd) having the opposite chirality.

The transition enthalpies  $\Delta H_{\text{c}}$  listed in the 4th column of Table 1 were calculated according to the zipper model for various combinations of  $\sigma$  and  $s$ . In most cases, the observed transition curves were found to be reproduced equally well by using  $\sigma$  values in the range 0–1. In consideration of the experimental DSC data of PPLA [40], the results of calculations are shown for two values of  $\sigma$  (0.0001 and 0.001) in the 4th column of Table 1. Also listed in the table are the transition temperature  $T_{\text{c}}$  and van't Hoff energy (expressed in kJ/mol of polymers) obtained directly from the experimental transition curve. In the range  $\sigma < 0.0001$ , the value of  $\Delta H_{\text{c}}$  remains nearly invariant. For copolymers involving BLA residues, the  $\Delta H_{\text{c}}$  values tend to be somewhat smaller than those from homopolymer PPLA.

Shown in Table 2 are the summary of the analysis of the experimental data collected in the dilute, isotropic TCE solution. Three different techniques such as  $^1\text{H}$  NMR, FTIR, and ORD ( $b_0$ ) were employed to follow the transition behaviors of PPLA. As noted in the preceding paper [19], the  $^1\text{H}$  NMR measurements were hampered by the low solubility of PPLA at lower temperatures: the transition curve thus derived was found to be less steep than those from the other measurements. For given polymers, the slope

of the thermal transition curve becomes moderate in the isotropic state [35]. These observations are reflected in the lower values of the van't Hoff energy  $\Delta H_{\text{v}}$  in Table 2 relative to those in Table 1. Nevertheless the transition temperatures  $T_{\text{c}}$  remain nearly unaffected regardless of whether the solution is isotropic (Table 2) or liquid crystalline (Table 1), suggesting that the transition mechanism is more or less identical.

As indicated in Table 2, larger  $\sigma$  values (0.01 and 0.1) are adopted for the isotropic dilute solution. Use of the same  $\sigma$  values (0.0001–0.001) as in Table 1 leads to much lower estimates of  $\Delta H_{\text{c}}$  than those of the experimental enthalpy change (1.6 kJ/mol) of PPLA [40]. The difference in  $\sigma$  values may be attributable to a higher chain flexibility in the dilute solution. Copolymerization with BLA up to 24% does not affect the value of  $\Delta H_{\text{c}}$  for a given  $\sigma$  value (4th–6th rows of Table 2). The  $\Delta H_{\text{c}}$  value obtained for Copoly (49BLA- $\beta_{\text{Rd}}$ -ran-51PLA) tends to be much lower however (the bottom row). The physical meaning of the instability factor  $\sigma$  will be further examined in the following sections.

#### 4. The effect of the instability factor $\sigma$

In the present theoretical framework, we cannot offer any reasonable way to determine the magnitude of the instability factor  $\sigma$ . Under such circumstances, the most probable  $\sigma$  value may be selected in consideration of the experimental  $\Delta H_{\text{c}}$  data. The  $\Delta H_{\text{c}}$  values of PPLA shown in Table 1 fall in the range of the enthalpy change  $\Delta H$  associated with the thermal transition of PPLA in the LC state in TCE. For copolymers with BLA, as one may expect, the values of  $\Delta H_{\text{c}}$  derived for the LC state tend to be lower than those of the homopolymer. The reliable estimate of  $\Delta H$  becomes more difficult in the isotropic dilute solution (Table 2). When chains are isolated in a dilute solution, the  $\alpha$ -helical backbone may gain higher flexibility: a larger disorientation at the  $\ell/r$  junction may facilitate the transition, and lead to a larger  $\sigma$  value than those assumed in the LC state. Adoption of a higher value of  $\sigma$  enhances the magnitude of  $\Delta H_{\text{c}}$ , but never to the range of those listed in Table 1 for the LC state.

To examine the effect of  $\sigma$  at given DPs, calculations were tentatively carried out for two representative sets of experimental data: PPLA (E1) and copoly(49BLA- $\beta_{\text{Rd}}$ -ran-51PLA) obtained in the LC state. For given sets of  $\sigma$  and  $n$ ,  $\Delta H_{\text{c}}$  values were so adjusted as to reproduce the experimental observations. Fig. 4 indicates variation of  $\Delta H_{\text{c}}$  with  $\sigma$  and  $n$ . Two  $\sigma$  values are examined: i.e., 0.0001 (cf. Table 1) and 0.01 (cf. Table 2). The  $\Delta H_{\text{c}}$  value decreases rapidly in the range  $n < 200$ , but tends to be moderate around  $n = 300$  for given values of  $\sigma$ . The DP of the polymers and copolymers used in the experiments [19,31] remain mostly in this range. The effect of  $\sigma$  is appreciable for all  $n$ . At  $n = 300$ , the values of  $\Delta H_{\text{c}}$  are depressed by about 1.5 and 1.0 kJ/mol respectively for PPLA (E1) and copoly (49BLA- $\beta_{\text{Rd}}$ -ran-51PLA) with reduction in  $\sigma$  from 0.01 to 0.0001. Taking the observed heat of transition into account, the former  $\sigma$  value

**Table 1**

Transition enthalpies elucidated from the  $^2\text{H}$  NMR data in TCE in the nematic LC state:  $\Delta H_{\text{v}}$  from the van't Hoff relation and  $\Delta H_{\text{c}}$  for the zipper model with  $n = 300$ .

Sample	$T_{\text{c}}$ (°C)	van't Hoff $\Delta H_{\text{v}}$ (kJ/mol)	Zipper model		Ref.
			$\sigma = 0.0001$	(0.001)	
PPLA- $\beta_{\text{Rd}}$ (E1)	83.2	656.2	2.21	(2.42)	[31]
PPLA- $\beta_{\text{Rd}}$ (E2)	82.8	767.2	2.59	(2.82)	[31]
PPLA- $\beta_{\text{Rd}}$ in PBLG	86.6	503.0	1.69	(1.85)	[31]
Copoly(22BLA- $\beta_{\text{Rd}}$ -ran-78PLA- $\beta_{\text{Rd}}$ )	71.0	310.7	1.05	(1.14)	[31]
Copoly(22BLA- $\beta_{\text{Rd}}$ -ran-78PLA)	70.4	343.7	1.16	(1.27)	[31]
Copoly(24BLA- $\beta_{\text{Rd}}$ -ran-76PLA)	76.1	224.6	0.76	(0.83)	[19]
Copoly(49BLA- $\beta_{\text{Rd}}$ -ran-51PLA)	37.2	418.7	1.41	(1.54)	[19]

**Table 2**

Transition enthalpies elucidated from the data observed in TCE in a dilute isotropic state:  $\Delta H_{\text{v}}$  from the van't Hoff relation and  $\Delta H_{\text{c}}$  for the zipper model with  $n = 300$ .

Sample	$T_{\text{c}}$ (°C)	van't Hoff $\Delta H_{\text{v}}$ (kJ/mol)	Zipper model		Ref.
			$\sigma = 0.01$	(0.1)	
PPLA ( $^1\text{H}$ NMR) <sup>a</sup>	87.6	159.0	0.93	(1.57)	[19]
PPLA (FTIR)	82.1	234.0	1.46	(2.70)	[41]
PPLA (ORD, $b_0$ )	90.7	188.4	1.09	(1.86)	[19]
Copoly(09BLA- $\beta_{\text{Rd}}$ -ran-91PLA) (ORD, $b_0$ )	83.9	174.8	1.02	(1.73)	[19]
Copoly(24BLA- $\beta_{\text{Rd}}$ -ran-76PLA) (ORD, $b_0$ )	66.7	192.4	1.12	(1.90)	[19]
Copoly(49BLA- $\beta_{\text{Rd}}$ -ran-51PLA) (ORD, $b_0$ )	41.4	107.9	0.63	(1.06)	[19]

<sup>a</sup> As noted in Ref. [19], the  $^1\text{H}$  NMR measurements are hampered by the low solubility of PPLA in TCE at lower temperatures.

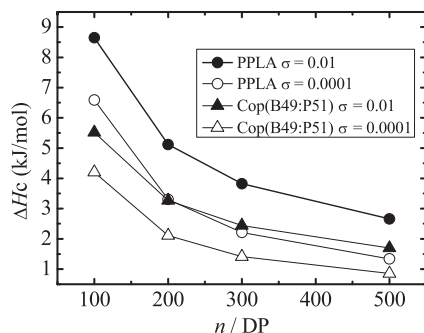


**Fig. 4.**  $n$ -dependence of  $\Delta H_c$  for PPLA- $\beta_{Rd}$  (circles) and Copoly(49BLA- $\beta_{Rd}$ -ran-51PLA) (triangles) derived from the analysis of  $^2\text{H}$  NMR data in the LC state, estimated for two  $\sigma$  values as indicated in the diagram.

exceeds the upper limit for these polymers in the LC state. In the range  $\sigma < 0.0001$ , the effect on the  $\Delta H_c$  value becomes practically nil at  $n = 300$ . These considerations underlie the choice of  $\sigma$  values in Tables 1 and 2.

## 5. Discussion

As stated earlier (cf. Eq. (4)), the assumption of  $\sigma = 0.0$  entirely eliminates the intermediate fraction, leading to the equilibrium between the two chemical species, i.e., all- $r$  and all- $\ell$  form. This is the concept of the van't Hoff model. The values of  $\Delta H_c$  given in the 3rd column of Tables 1 and 2 correspond to this limit. The results of the analysis indicate that despite the thermodynamically unfavorable aspects of the  $\ell/r$  junction, there is a finite probability that a polymer molecule contains the transient configurations intervening between the two helical portions. The observed transitions have been successfully described by the two-parameter scheme set forth in this work. In the present treatment,  $\sigma$  is introduced as the instability parameter at the  $\ell/r$  junction which corresponds to the moving front of the zipper transition. In the conventional Zimm–Bragg model [27], the transition is assumed to take place through a multi-block intermediate state. The factor  $\sigma$  is then defined as the nucleation parameter associated with the extra free energy to create a junction at a given site along the chain. Experiments on the random copolymers of PLA and BLA strongly suggest that the transition proceeds through a single-front-moving mechanism [19]. The characteristics of the  $\sigma$  parameter appreciably differ from those customarily adopted for the helix–coil transition.

Nevertheless the role of  $\sigma$  in the mathematic operation is similar to that originally introduced in the treatment of the helix–coil transition [27]. Following the argument presented by Applequist [42], the instability parameter may be understood as an equilibrium constant for the formation of an interruption

$$\sigma = \exp(-\Delta G_0/RT) \quad (9)$$

where  $\Delta G_0$  is the extra free energy of the  $\ell/r$  junction formation. Since the number of H-bonds remains constant during the transition process, the energy contribution ( $\Delta H_0$ ) may be insignificant. Thus

$$\sigma \approx \exp[(\Delta S_0/R)] \quad (10)$$

where  $\Delta S_0$  accounts for the entropy change to create an interruption for the rearrangement of H-bonds. The intermediate state involves at least 3 monomeric residues or four hydrogen bonds to complete the reversal of the  $\alpha$ -helical screw-sense. Let  $\sigma = 0.001$ , Eq. (9) leads to  $\Delta S_0 \approx -57$  J/mol K, or  $\Delta S_0/3 \approx -19$  J/mol K for a residue. Adoption of a larger  $\sigma$  value (0.01) from the isotropic solution yields  $\Delta S_0 \approx -38$  J/mol K, or  $\Delta S_0/3 \approx -13$  J/mol K for

a residue. The entropy penalty to create an unfolded site is slightly higher in the LC state. Our interest is now to elucidate the chain configuration at the transition site. A RIS simulation has been attempted and results were reported in the literature [34,35]. In the range of  $\sigma$  estimated above, however, the fraction of the junction sites seems to be so low that they may easily elude experimental observations. In spite of such experimental difficulties, it may be worth investigating the  $\Delta H_c$ – $\sigma$  relation for copolymers of higher BLA content (>50%).

Eq. (1) is a standard thermodynamic expression for the temperature-dependence of the free-energy difference between the two states. While the front factor  $A = \Delta H_c/RT_c$  is responsible for the slope of the  $\ln s$  vs.  $T$  relation, the succeeding term  $(1 - T_c/T)$  takes care of the thermal variation of  $\ln s$  in terms of reduced temperature. It is important to note that the characteristics of the individual polymer systems are included in term  $A$ . Variation of  $T_c$  as a function of PLA content of copolymers is previously shown in Fig. 11 of the preceding paper. In contrast to  $T_c$ , the accurate estimate of the steepness of the transition curves is difficult, and thus  $\Delta H_c$  values listed in Tables 1 and 2 inevitably involve larger uncertainty. Nevertheless, it should be interesting to examine how  $A$  varies with the copolymer composition. In Fig. 5, the  $A$  values elucidated from the IR and  $b_0$  measurements in the dilute isotropic solution (Table 2) are plotted against the PLA content of copolymers. With the reason stated earlier (cf. Section 3), the  $A$  value derived from  $^1\text{H}$  NMR measurements is omitted from the plot. The general trend of the plot is followed by a linear fitting. A long extrapolation to PLA content = 0 yields  $A = 0.09$ , suggesting that the magnitude of  $\Delta H_c/RT_c = \Delta S_c/R$  declines toward the PBLA limit. The values of  $A$  obtained from Table 1 for the LC state are somewhat larger, and when plotted, the points are more scattered. The decrease in  $A$  illustrated in Fig. 5 is consistent with the observation that PBLA takes the  $\ell$ -form in conventional helicoidal solvents at room temperature [9–12], and easily transforms into the coil state by addition of a small amount of organic acids [43,44]. Such vulnerability of the PBLA system is strongly related to the smaller free-energy difference between the two chiral states. In our model, the average values of the side-chain conformation energy should be approximately proportional to the copolymer composition. The screw-sense of copolymers remains in the  $\ell$ -regime below PLA content = ca. 0.4 at room temperature (cf. Fig. 3 of the preceding paper).

As shown in Scheme 1, PPLA also exhibits an inverse-type helix–helix transition in a mixed solvent such as TCE/TFA. The rotational characteristics of bond  $\chi_1$  are sensitively affected by the presence of an organic acid (TFA). According to the  $^1\text{H}$  NMR observations [16,18], the fraction of the gauche conformation ( $\chi_1$ ) tends to be higher with increasing acid concentration or alternatively with decreasing temperature. The free-energy change in the side-chain conformation triggers the screw-sense inversion of  $\alpha$ -helix from the  $r$ - to  $\ell$ -form with descending temperature.

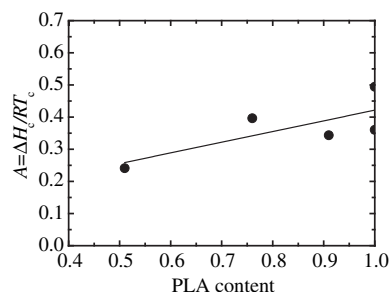


**Fig. 5.** Variation of  $A = (\Delta H_c/RT_c)$  with PLA content.

Essentially the same mechanism may be assumed for the inverse-type transition as long as the H-bond network along the  $\alpha$ -helical backbone is effectively maintained. As temperature is further lowered, the solution becomes biphasic where the  $\alpha$ -helical  $\ell$ -form is in equilibrium with the coil state [18] (cf. Scheme 1).

## 6. Concluding remarks

It would be interesting to examine the effect of residues other than aspartates. Inclusion of a few mol% of BLG residue as a comonomer is enough to prevent the completion of the screw-sense inversion of PPLA [31]. According to the previous analysis of the side-chain conformation, the  $\chi_1$  bond of PLA is very susceptible to temperature or polarity of solvent. The origin of such flexibility may be traced back to the chemical constitution of the  $\chi_1$  bond. When a C–C bond carries polarizable groups on both sides, the energy difference between the *t* and *g* states tends to be lowered, and often a pronounced gauche preference (a gauche effect) is detected [45,46]. Since BLG includes another methylene unit between  $C_\alpha$  and the ester carbonyl group, no such gauche-stabilization effect can be expected. While the PLA side chain gains more freedom in the high-temperature  $\ell$ -form by taking a  $\chi_1 = g^-$  arrangement, BLG stubbornly prefers an extended  $\chi_1 = t$  conformation [47]. Our observation is consistent with the results of Bradbury et al. [48] who examined the compatibility of BLA with the two isomers of  $\gamma$ -benzyl glutamate by preparing the random copolymer. While copolymers with the *D*-isomer ( $\ell$ -preference) remain in the  $\ell$ -form over the entire composition, the helical sense of the copolymer with the *L*-isomer (*r*-preference) is largely determined by the glutamate residue and the  $b_0$  value remained below  $-400$  over the range of BLA content = 0–85%.

PPLA is known to exhibit an irreversible screw-sense inversion from the *r*- $\alpha$ -helix to  $\ell$ - $\pi$ -helix in the solid state at about 130°C [24]. Luijten et al. [49] have reported a reversible transition in PPLA films end-grafted on silicon or quartz substrates: the original *r*- $\alpha$ -helix has been recovered from the high-temperature  $\pi$ -helix by immersion in chloroform. It is of interest to note that a racemic mixture of PPLA with its optical antipode PPDA undergoes a reversible transition to the high-temperature  $\alpha$ -form at about 200°C [31]. In polyaspartates having somewhat longer side chains, a similar transition takes place reversibly in the solid state [50–54]. These observations are quite consistent with the zipper-type mechanism of the screw-sense inversion described above. Detailed studies on the mechanism of the screw-sense inversion in the solid state are in progress in our laboratory.

## Acknowledgment

This work was partially supported by the Private University Frontier Research Center Program sponsored by the Ministry of Education, Culture, Sports, Science and Technology (Monbukagakusho). The financial support by a Grant-in-Aid for Science Research (18550111) of Monbukagakusho (A.A.) is also acknowledged.

## References

[1] Blout ER, Karlson RH. *J Am Chem Soc* 1958;80:1259–60.

- [2] Karlson RH, Norland KS, Fasman GD, Blout ER. *J Am Chem Soc* 1960;82:2268–75.
- [3] In his pioneering work, Malcolm [4,5] has found that high molecular weight PBLA forms a right-handed  $\alpha$ -helix when spread as a monolayer at the air-water interface and remains stable in dried collapsed films. Later Riou, et al. [6] confirmed that the right-handed  $\alpha$ -helices are formed on the surface of water immediately after spreading the monolayers, independently of the conformational distribution in the spreading solution. Giacotti et al. [7] have reported that the preferred form of high molecular weight PBLG is right-handed in trimethyl phosphate at room temperature. According to Kyotani et al. [8], a slow transformation from the  $\ell$ - to *r*-form has been observed by exposure to a humidified chloroform vapor.
- [4] Malcolm BR. *Nature* 1968;219:929–30.
- [5] Malcolm BR. *Biopolymers* 1970;9:911–22.
- [6] Riou SA, Hsu SL, Stidham HD. *Biophys J* 1998;75:2451–60.
- [7] Giacotti V, Quadrifoglio F, Crescenzi V. *J Am Chem Soc* 1972;94:297–8.
- [8] Kyotani H, Kanetsuna H, Oya M. *J Polym Sci Part B Polym Phys* 1977;15:1029–36.
- [9] Goodman M, Deber CM, Felix AM. *J Am Chem Soc* 1962;84:3773–4.
- [10] Bradbury EM, Carpenter BG, Goldman H. *Biopolymers* 1968;6:837–50.
- [11] Bradbury EM, Carpenter BG, Stephens RM. *Biopolymers* 1968;6:905–15.
- [12] Toniolo C, Falxa ML, Goodman M. *Biopolymers* 1968;6:1579–603.
- [13] Toriumi H, Saso N, Yasumoto Y, Sasaki S, Uematsu I. *Polym J* 1979;11:977–81.
- [14] Tsujita Y. *Biophys Chem* 1988;31:11–20.
- [15] Tsujita Y, Watanabe T, Takizawa A, Kinoshita T. *Polymer* 1991;32:569–75.
- [16] Abe A, Hiraga K, Imada Y, Hiejima T, Furuya H. *Biopolymers (Peptide Science)* 2005;80:249–57.
- [17] Abe A, Imada Y, Hiejima T, Furuya H. In: Blondelle SE, editor. *Understanding biology using peptides*. American Peptide Society; 2005. p. 700–1.
- [18] Abe A, Imada Y, Hiejima T, Furuya H. *Chem Today* 2006;24:52–4.
- [19] Imada Y, Abe A. The preceding paper.
- [20] Teramoto A. *Seibutsu Butsuri* 1973; 13:149–163.
- [21] McKnight RP, Karasz FE. *Macromolecules* 1974;7:143–5.
- [22] Teramoto A, Fujita H. *Adv Polym Sci* 1975;18:65–149.
- [23] Dupré DB. *Biopolymers* 1990;30:1051–60.
- [24] Sasaki S, Yasumoto Y, Uematsu I. *Macromolecules* 1981;14:1797–801.
- [25] Abe A. In: Kahovec J, editor. *Macromolecules*. Utrecht: VSP; 1992. p. 221–8. 1993.
- [26] Pauling L, Corey RB, Branson HR. *Proc Natl Acad Sci USA* 1951;37:205–11.
- [27] Zimm BH, Bragg JK. *J Chem Phys* 1959;31:526–35.
- [28] Nagai KJ. *Phy Soc Jpn* 1960;15:407–16.
- [29] Lifson L, Roig A. *J Chem Phys* 1961;34:1963–74.
- [30] Abe A, Okamoto S, Kimura K, Tamura K, Onigawara H, Watanabe J. *Acta Polym* 1993;44:54–6.
- [31] Okamoto S. Ph.D. Dissertation: Tokyo Institute of Technology; 1995.
- [32] Abe A, Furuya H, Okamoto S. *Polym Sci Ser A* 1996;38:317–23. from *Vysokomol Soedin Ser A* 1996; 38: 566–573.
- [33] Abe A. *Makromol Symp* 1997;118:23–32.
- [34] Abe A, Furuya H, Okamoto S. *Biopolymers (Peptide Science)* 1997;43:405–12.
- [35] Okamoto S, Furuya H, Abe A. *Polym J* 1995;27:746–56.
- [36] Toriumi H. *Macromolecules* 1984;17:1599–605.
- [37] Prasad O, Sinha L, Gupta GP, Agnihotri RC, Misra N, Lal JN. *Polymer* 2005;46:7450–5.
- [38] Ushiyama A, Furuya H, Abe A, Yamazaki T. *Polym J* 2002;34:450–4.
- [39] Van't Hoff JH. *Études de Dynamique Chimique*. Amsterdam: Frederick Muller & Co.; 1884.
- [40] The values reported in Ref. [31] have been reconfirmed in this work.
- [41] Yamamoto T, Honma R, Nishio K, Hirotsu S, Okamoto S, Furuya H, et al. *J Mol Struct* 1996;375:1–7.
- [42] Applequist JJ. *Chem Phys* 1963;38:934–41.
- [43] Hayashi Y, Teramoto A, Kawahara K, Fujita H. *Biopolymers* 1969;8:403–20.
- [44] Norisuye T, Misumi K, Teramoto A, Fujita H. *Biopolymers* 1973;12:1533–41.
- [45] Orville-Thomas WJ, editor. *Internal rotation in molecules*. New York: Wiley; 1974.
- [46] Abe A, Furuya H, Mitra MK, Hiejima T. *Comp Theor Polym Sci* 1998;8:253–8.
- [47] Abe A, Yamazaki T. *Macromolecules* 1989;22:2138–45.
- [48] Bradbury EM, Downie AR, Elliott A, Hanby WE. *Proc Roy Soc (London)* 1960;A259:110–28.
- [49] Luijten J, Vorenkamp EJ, Schouten AJ. *Langmuir* 2007;23:10772–8.
- [50] Okamoto S, Furuya H, Watanabe J, Abe A. *Polym J* 1996;28:41–4.
- [51] Watanabe J, Okamoto S, Satoh K, Sakajiri K, Furuya H, Abe A. *Macromolecules* 1996;29:7084–8.
- [52] Sakajiri K, Satoh K, Kawauchi S, Watanabe J. *J Mol Struct* 1999;476:1–8.
- [53] Sakajiri K, Satoh K, Yoshioka K, Kawauchi S, Watanabe J. *J Mol Struct* 1999;477:175–9.
- [54] Sakajiri K, Saeki S, Kawauchi S, Watanabe J. *Polym J* 2000;32:803–6.